Investigation of Dose Calculation Accuracy of Eclipse Treatment Planning System in the Presence of Metal Hip Prosthesis with Thermoluminescence Dosimeters[*]

Osman Vefa GÜL[**], Hamit BAŞARAN[***], Ahmet YILDIRIM[****], Gökçen İNAN[*****]

Abstract

Aim: This study investigated the dose calculation accuracy of different treatment planning algorithms used in radiotherapy patients with hip prostheses.

Method: The current research produced a tissue-equivalent cylindrical phantom that imitates a leg using a 3D printer. Co-Cr-Mo alloy and Ti-6AI-4V alloy prostheses were placed in the centre of the phantom, respectively. Both prostheses' dose measurements were taken with thermoluminescent dosimeters (TLD) at 92 points. The dose calculation accuracy of the Analytical Anisotropic Algorithm (AAA) and Pencil Beam Convolution (PBC) algorithms, widely used in radiotherapy, were compared with the measurement results.

Results: Since the Co-Cr-Mo hip prosthesis has a high density, the number of backscattered photons around it was higher than the Ti-6AI-4V hip prosthesis. The average surface dose of the Co-Cr-Mo alloy was 364.05 cGy, while the average surface dose of the Ti-6AI-4V alloy was 347.79 cGy.

Conclusion: It was observed that the dose estimation abilities of the AAA and PBC algorithms decreased as the density of the hip replacement increased. In addition, the AAA algorithm predicted the surface dose in the phantom better than the PBC algorithm.

Keywords: Hip prosthesis, radiotherapy, thermoluminescent dosimetry, algorithms.

Özgün Araştırma Makalesi (Original Research Article)
Geliş / Received: 06.12.2023 & **Kabul / Accepted:** 13.03.2024
DOI: https://doi.org/10.38079/igusabder.1401159
[*] This study was supported by the Scientific Research Projects (BAP) Grants Unit, Selcuk University, Konya, Türkiye. [Grant Number: 21401102].
[**] Corresponding Author, Asst. Prof. Dr., PhD., Department of Radiation Oncology, Faculty of Medicine, Selcuk University, Konya, Türkiye. E-mail: vefagul@selcuk.edu.tr ORCID https://orcid.org/0000-0002-6773-3132
[***] Assoc. Prof. Dr., MD., Department of Radiation Oncology, Faculty of Medicine, Selcuk University, Konya, Türkiye. E-mail: drhamitbasaran@gmil.com ORCID https://orcid.org/0000-0002-2122-8720
[****] Assoc. Prof. Dr., MD., Department of Orthopaedics and Traumatology, Faculty of Medicine, Selcuk University, Konya, Türkiye. E-mail: droto@yandex.com ORCID https://orcid.org/0000-0002-3953-091X
[*****] Department of Radiation Oncology, Faculty of Medicine, Selcuk University, Konya, Türkiye. E-mail: gokceninan85@gmail.com ORCID https://orcid.org/0000-0003-2995-0256

Metal Kalça Protezi Varlığında Eclipse Tedavi Planlama Sisteminin Doz Hesaplama Doğruluğunun Termolüminesans Dozimetreler ile Araştırılması

Öz

Amaç: Bu çalışmada kalça protezi olan radyoterapi hastalarında kullanılan farklı tedavi planlama algoritmalarının doz hesaplama doğruluğu araştırıldı.

Yöntem: Bu çalışmada 3D yazıcı kullanılarak bacağı taklit eden doku eşdeğeri silindirik bir fantom üretildi. Fantomun merkezine sırasıyla Co-Cr-Mo alaşımı ve Ti-6AI-4V alaşımı protezler yerleştirildi. Her iki protezin doz ölçümleri 92 noktada termolüminesan dozimetreler (TLD) ile alınmıştır. Radyoterapide yaygın olarak kullanılan Analitik Anizotropik Algoritma (AAA) ve Pencil Beam Convolution (PBC) algoritmalarının doz hesaplama doğruluğu ölçüm sonuçları ile karşılaştırıldı.

Bulgular: Co-Cr-Mo kalça protezi yüksek yoğunluğa sahip olduğundan, etrafına geri saçılan foton sayısı Ti-6AI-4V kalça protezinden daha yüksekti. Co-Cr-Mo alaşımının ortalama yüzey dozu 364.05 cGy iken, Ti-6AI-4V alaşımının ortalama yüzey dozu 347.79 cGy idi.

Sonuç: AAA ve PBC algoritmalarının doz tahmin yeteneklerinin kalça protezinin yoğunluğu arttıkça azaldığı gözlendi. Ayrıca AAA algoritması fantomdaki yüzey dozunu PBC algoritmasına göre daha iyi tahmin etti.

Anahtar Sözcükler: Kalça protezi, radyoterapi, termolüminesan dozimetri, algoritmalar.

Introduction

Complaints of osteoarthritis, severe pain, and limitation of movement are common in the elderly population, which increases with the prolongation of the average life expectancy. Total hip replacement surgery is applied to increase the daily living activities of individuals[1]. The total hip replacement consists of two main parts. The first is the acetabular part placed in the pelvis, and the second is the femoral part placed inside the leg bone[2]. Co-Cr-Mo and Ti-6AI-4V alloys are the commonly used hip prostheses[3]. These materials have high atomic numbers and adversely affect their dose distribution. In radiotherapy, the effect of high-density prostheses on dose distribution is of great importance. The prosthesis can cause striated image artefacts and complicate dose calculations for nearby organs in patients with high electron-density hip replacements[4-6]. 4% of patients who need radiotherapy have metallic implants. Among these patients, hip replacement has an important place. AAPM Task Group 63 stated that the gantry angles where the prosthesis does not enter the beam area should be selected first. In addition, the AAPM Task Group 63 reported that algorithms used in treatment planning systems (TPS) fail to predict doses around high atomic number prostheses. In the presence of high atomic number prostheses, this failure of TPS in dose estimation may

adversely affect the treatment of patients[7]. As a result of rapid developments in TPS, the predictive ability of dose calculation algorithms is increasing. The Pencil Beam Convolution (PBC) algorithm, which is one of the model-based algorithms, is obtained as a result of the integration of all point spread kernels along the infinite beam path of the photons in the phantom[8]. The Analytical Anisotropic Algorithm (AAA) model provides fast and accurate dose calculation for photon beams, even in regions with complex tissue heterogeneities. The AAA dose calculation algorithm can successfully calculate primary photons, scattered out-of-focus photons, and electrons scattered from beam-regulating devices. PBC and AAA algorithms are widely used in radiotherapy clinics[9]. The PBC and AAA algorithms do not fully account for rays passing through metallic implants and underestimate the dose reduction[10]. Many authors have studied the effect of high-density materials on radiation therapy. However, no study in the literature compares the dose calculation accuracy of AAA and PBC algorithms with thermoluminescence dosimetry (TLD) dose measurements in the presence of different hip prostheses.

This study investigated the effects of Co-Cr-Mo and Ti-6AI-4V alloys used as hip prostheses on dose distribution. The accuracy of dose distributions calculated with AAA and PBC algorithms was compared with TLD measurements.

Material and Methods

Hip Prostheses

The current study used Co-Cr-Mo and Ti-6AI-4V alloys as hip prostheses. The Co-Cr-Mo alloy hip prosthesis is manufactured to the standard specification for cast alloy (UNS R30075) for Cobalt-28 Chromium-6 Molybdenum alloy prosthesis and surgical implants. The Ti-6AI-4V alloy hip implant is manufactured to ISO 5832-3:2016 standards. Both prostheses ' stem size and length were 12 mm and 150 mm, respectively. Both prostheses were divided into three parts by thickness. Electron density relative to water of Co-Cr-Mo and Ti-6AI-4V hip implants relative was 6.89 g/cm^3 and 3.76 g/cm^3, respectively. The positions of Co-Cr-Mo and Ti-6AI-4V hip implants in the phantom are shown in Fig. 1.

Figure 1. Co-Cr-Mo and Ti-6AI-4V hip prostheses

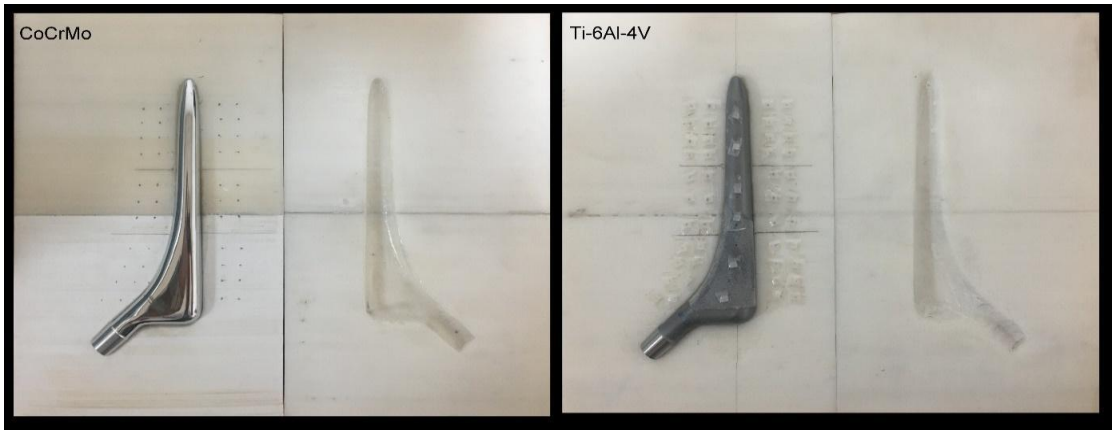

Phantom

This study used a cylindrical phantom with a hip prosthesis in the center, as shown in Fig. 2. The phantom was created by a 3D printer using an acrylonitrile butadiene styrene (ABS) filament. The density of the produced phantom was 1.04 gr/cm^3. The dimensions of the phantom were designed as X=150 mm, Y=150 mm, and Z=250 mm. TLDs were placed along the X and Y axes as shown in figure 2. Before the computed tomography (CT) images were taken, the prosthesis in the phantom centre was divided into three thicknesses: thick, medium, and thin, respectively. Within the phantom, 44 TLD positions were determined on the X-axis along the length of the prosthesis. Measurement points determined along the X-axis were 1 cm and 2 cm from the prosthesis. For each part of the prosthesis, the points on the upper and lower surfaces were identified as A and E, respectively. The distances of B and F points from the prosthesis were 1.5 cm, 1.7 cm, and 1.9 cm for parts 1, part 2, and part 3, respectively. The distances of C and G points from the prosthesis were 4 cm, 4.2 cm, and 4.4 cm for parts 1, part 2, and part 3, respectively. D and H points were located on the phantom surface. The distances of D and H points from the hip prosthesis were 6 cm, 6.2 cm, and 6.4 cm for parts 1, part 2, and part 3, respectively. CT images of the phantom were obtained with a 1 mm section thickness on the Toshiba Aquilion CT device and transferred to the TPS.

Figure 2. Cylindrical phantom with the hip prosthesis in the center

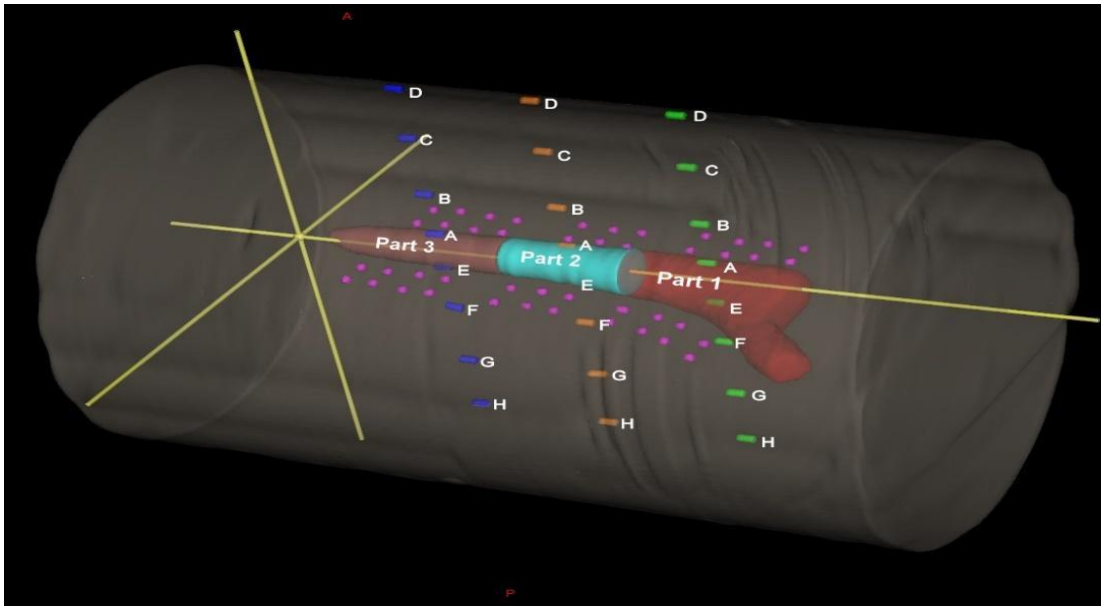

Contouring and Treatment Planning

The CT images of the two prostheses were transferred to Eclipse v15.1 TPS with AAA algorithm and Eclipse v8.6 TPS with PBC algorithm (Varian Medical Systems, Palo Alto, CA, USA). In this study, radiation therapy was taken as a reference after prosthesis replacement of patients who underwent arthroplasty due to a malignant tumour or metastasis in the femur. The replaced femoral head was defined as gross tumour volume (GTV). Clinical tumour volume (CTV) was created by giving a 1 cm margin to the GTV. The planned tumour volume (PTV) was defined by giving a 0.5 cm margin to the CTV. The mean Hounsfield units (HU) values calculated by Eclipse TPS for the Co-Cr-Mo and Ti-6AI-4V hip prostheses were 21000 and 8600, respectively. The phantom was irradiated with 6 MV from 0 and 180 angles of the gantry. Source Skin Distance (SSD) was 92.5 cm for both gantry angles. Four hundred monitor units (MU) were given, 200 MU for each angle. MLCs for each beam field were positioned to give a 0.75 cm margin to the PTV. Dose calculations were made in AAA and PBC algorithms. Dose measurements were made with TLDs at 92 measurement points determined.

Phantom Irradiations and TLD Dose Measurement

The necessary calibration was performed on the Varian DHX linear accelerator device to give one cGy per MU at dmax depth for 6 MV. The accuracy of the phantom's position

was ensured by taking the radiographic films (port films). Plans for both prostheses were applied to the phantom via the linear accelerator device. This study used 92 TLD-100s with 3.2 mm x 3.2 mm x 0.9 mm chip shapes obtained by doping natural lithium fluoride (LiF) with Mg and Ti. TLDs were calibrated in Varian DHX linear accelerator device using 6 MV energy. The calibration conditions were such that the source-skin distance (SSD) was 100 cm, and 1Gy was received at a field size of 10 cm x 10 at a depth of 1.5 cm from the surface. The same positioning of the TLDs in the phantom was ensured according to the measurement points marked before the CT. TLDs' Calibration curves for measurement were drawn between 5 cGy and 400 cGy. The calibration curve is given in Fig. 3. TLDs were annealed at 400°C for 1 hour and at 100°C for 2 hours before measurements. Before reading, the irradiated TLDs were annealed at 100°C for 10 minutes to eliminate the rapidly decreasing luminescence peaks. A Harshaw 3500 TLD reader (ThermoFisher Scientific) was used to read the TLDs. Measurements were repeated three times for each hip prosthesis irradiation, and the mean dose was calculated. The point dose measured by TLDs and the dose calculated by TPS were compared for each point.

Figure 3. TLD-100 calibration curve

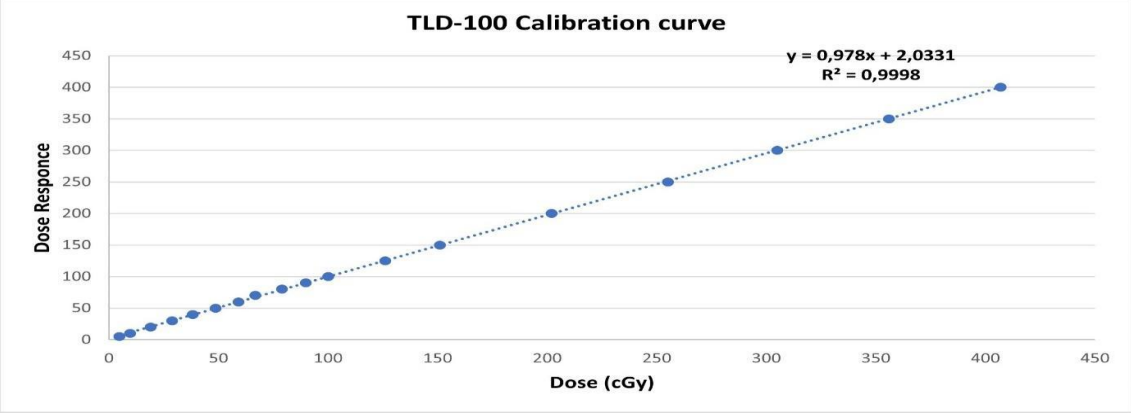

Analysis of the Results

Evaluation of values measured by TLDs and calculated by TPS was performed according to TRS 430 protocol (IAEA., 2008). According to this protocol, the difference between TPS dose calculation algorithms and doses measured by TLDs is defined as:

$\delta\ (\%) = 100*(D_{TPS}-D_{TLD})/D_{TLD}$

δ (%) represents the percent error. D_{TPS} represents the dose calculated by TPS, and D_{TLD} represents the dose measured by TLD. The percent error between TPS and TLD doses was defined for 92 points determined in the phantom.

Results

TPS and TLDs obtained dose distribution for Co-Cr-Mo and Ti-6AI-4V alloy prostheses. The calculated and measured doses for the prostheses' thick, medium and thin parts are given in Table 1, Table 2 and Table 3, respectively. It was observed that the density and thickness of the hip prosthesis directly affected the dose distribution. The average surface dose of the Co-Cr-Mo alloy was 364.05 cGy, while the average surface dose of the Ti-6AI-4V alloy was 347.79 cGy. It was observed that the dose estimation performances of AAA and PBC algorithms decreased as the density of the hip prosthesis increased. It was observed that the PBC algorithm was more successful than the AAA algorithm in calculating the dose along the Y-axis for the Co-Cr-Mo alloy. However, the AAA algorithm more successfully calculated the dose along the X-axis. It was seen that the AAA algorithm was more successful than the PBC algorithm in calculating the dose along the Y-axis for Ti-6AI-4V alloy. The results of the two algorithms were similar for dose estimation along the X-axis. It has been observed that the density of the hip prosthesis affects the dose on the phantom surface at a distance of 7.5 cm. It was also found that the AAA algorithm predicted the surface dose in the phantom better than the PBC algorithm.

Table 1. Comparison of doses calculated by TPS and TLDs for the hip prosthesis's thick part (part 1).

Position		**Calculated dose**		**Measured dose**	**Percentage difference**	
		AAA	**PBC**		**Meas./AAA**	**Meas./PBC**
Co-Cr-Mo Alloy	**D**	168.90±0.86	148.86±0.72	192.90±5.31	-12.44	-22.83
	C	332.20±5.37	339.80±0.54	344.80±0.22	-3.65	-1.45
	B	316.95±3.67	332.85±0.16	343.20±0.88	-7.65	-3.02
	A	313.40±2.74	333.70±0.33	359.27±5.49	-12.77	-7.12
	E	311.95±2.68	334.50±0.44	355.30±0.33	-12.20	-5.85
	F	317.85±3.01	332.95±0.38	343.00±0.11	-7.33	-2.93
	G	329.50±2.74	338.35±0.05	344.95±0.55	-4.48	-1.91
	H	169.92±0.80	149.10±0.68	198.57±0.65	-14.43	-24.91
	X(1cm)	353.60±4.53	368.39±4.39	359.83±6.27	-1.73	2.38

	X(2cm)	327.85±15.98	356.01±7.59	341.52±6.82	-4.00	4.24
Titanium Alloy	**D**	183.17±1.50	164.87±0.14	189.73±0.64	-3.46	-13.10
	C	350.15±2.03	354.45±0.55	339.33±7.33	3.19	4.46
	B	341.10±0.11	349.65±0.55	319.40±2.64	6.79	9.47
	A	338.77±0.90	353.87±0.80	347.18±5.94	-2.42	1.93
	E	337.53±0.49	353.47±0.10	333.17±5.66	1.31	6.09
	F	339.25±0.27	349.70±0.11	317.70±2.52	6.78	10.07
	G	348.15±0.38	354.30±0.33	328.15±2.03	6.09	7.97
	H	182.53±1.02	159.22±0.96	190.50±0.55	-4.18	-16.42
	X(1cm)	369.68±4.85	370.58±3.64	394.80±6.03	-6.36	-6.13
	X(2cm)	357.53±9.41	346.97±10.27	379.41±12.64	-5.77	-8.55

Table 2. Comparison of doses calculated by TPS and TLDs for the hip replacement's medium part (part 2).

Position		**Calculated dose**		**Measured dose**	**Percentage difference**	
		AAA	**PBC**		**Meas./AAA**	**Meas./PBC**
Co-Cr-Mo Alloy	**D**	182.17±0.68	167.89±0.42	201.83±4.83	-9.74	-16.82
	C	354.70±2.85	361.55±1.92	362.50±0.55	-2.15	-0.26
	B	347.55±2.03	356.10±1.31	348.45±0.60	-0.26	2.20
	A	339.30±0.66	359.75±1.37	366.25±0.84	-7.36	-1.77
	E	332.20±1.31	359.50±1.64	356.43±1.44	-6.80	0.86
	F	348.60±1.75	355.80±1.97	347.85±0.16	0.22	2.29
	G	355.35±2.03	360.55±2.25	356.55±0.49	-0.34	1.12
	H	182.75±0.88	168.24±0.53	203.56±0.50	-10.22	-17.35
	X(1cm)	364.20±5.14	370.55±4.71	365.60±7.45	-0.38	1.35
	X(2cm)	336.10±6.19	348.95±3.18	332.22±6.49	1.17	5.04
Titanium Alloy	**D**	184.50±0.55	176.33±0.44	194.37±1.89	-5.08	-9.28
	C	355.35±3.34	358.25±1.59	349.50±0.55	1.67	2.50
	B	348.35±3.23	353.65±1.70	339.93±1.88	2.48	4.04
	A	345.35±3.80	358.27±1.45	352.47±3.73	-2.02	1.65
	E	342.83±2.79	354.70±3.92	346.92±3.42	-1.18	2.24

	F	346.70±2.30	353.15±1.92	342.05±3.23	1.36	3.25
	G	353.95±2.13	358.00±2.19	349.75±0.27	1.20	2.36
	H	184.58±0.48	174.63±0.23	198.50±0.55	-7.01	-12.03
	X(1cm)	367.62±5.56	369.22±4.87	395.68±6.30	-7.09	-6.69
	X(2cm)	352.76±2.82	340.67±16.82	369.13±18.47	-4.43	-7.71

Table 3. Comparison of doses calculated by TPS and TLDs for the hip replacement's thin part (part 3).

Position		**Calculated dose**		**Measured dose**	**Percentage difference**	
		AAA	**PBC**		**Meas./AAA**	**Meas./PBC**
Co-Cr-Mo Alloy	**D**	188.77±0.61	175.71±0.83	201.63±2.71	-6.38	-12.86
	C	362.00±1.75	368.70±0.22	370.65±0.71	-2.33	-0.53
	B	352.25±0.49	363.10±0.11	360.05±1.04	-2.17	0.85
	A	350.25±1.59	365.50±0.55	376.16±0.55	-6.89	-2.83
	E	346.00±1.09	364.23±0.53	370.86±3.62	-6.70	-1.79
	F	352.75±0.27	362.25±0.05	359.10±0.11	-1.77	0.88
	G	360.75±0.16	367.50±0.22	363.33±5.09	-0.71	1.15
	H	189.62±0.60	176.35±1.12	204.07±0.18	-7.08	-13.58
	X(1cm)	365.06±5.85	373.30±5.22	368.25±3.29	-0.87	1.37
	X(2cm)	330.08±13.81	340.31±17.62	328.50±4.11	0.48	-3.47
Titanium Alloy	**D**	190.47±0.45	184.70±0.39	202.00±1.10	-5.71	-8.56
	C	361.35±2.25	365.65±1.26	360.10±3.83	0.35	1.54
	B	353.30±1.75	358.35±0.16	350.40±1.64	0.83	2.27
	A	346.20±0.11	363.20±0.11	356.67±6.47	-2.94	1.83
	E	349.45±1.59	362.30±0.55	350.35±0.38	-0.26	3.41
	F	352.20±1.20	358.65±0.38	348.06±1.60	1.19	3.04
	G	360.80±0.55	364.30±0.33	350.50±0.54	2.94	3.94
	H	193.83±1.69	185.20±1.69	201.00±1.10	-3.57	-7.86
	X(1cm)	365.23±5.79	370.15±4.32	395.23±2.29	-7.59	-6.35
	X(2cm)	352.86±2.75	340.83±10.41	359.38±10.75	-1.81	5.44

Discussion

Many authors have studied the effect of high-density materials on radiation therapy. However, no study compares the dose calculation accuracy of AAA and PBC algorithms with TLD dose measurements in the presence of different hip prostheses. In our study, the dose distribution at 92 different points around the hip prosthesis was measured with TLDs and the accuracy of the dose calculation algorithms was examined.

Paulu et al. designed a cylindrical phantom to evaluate the dose calculation accuracy of three common dose calculation algorithms used in two commercial treatment planning systems. A hip prosthesis was positioned in the centre of this phantom. They compared the TPS and TLD doses in the generated phantom. They determined the measurement points on the same X-axis as the hip prosthesis. According to the measurement results, it was found that the AAA algorithm underestimated the dose at the prosthesis interface by 6.11%-19.47% for the 6 MV photon energy[11]. In our current study, measurements were taken at 92 points on the X and Y axes for two different hip prostheses. For the Co-Cr-Mo alloy hip replacement, the difference between the doses calculated by the AAA algorithm along the Y-axis and the point doses measured by TLD was 3.65-14.43%, 0.22-10.22%, and 0.71-7.08% for part 1, part 2, and part 3, respectively. The difference along the x-axis was 1.73%-4.00%, 0.38-1.17% and 0.48-0.87% for Part 1, Part 2 and Part 3, respectively. Since the density of Ti-6AI-4V alloy is lower than that of Co-Cr-Mo alloy, the difference between AAA and TLD doses was at most 7.59%.

Ojala et al. in their study by placing a titanium implant inside the phantom, found that the Eclipse AxB algorithm underestimated the dose by 8-10%. They also stated that the AAA algorithm had higher dose inconsistency[12]. In our current study, the dose difference between Eclipse TPS and TLD doses was high for the thick part of the titanium implant. This dose difference was 6.79% and 16.42% for the AAA and PBC algorithms, respectively.

Le Fevre et al. investigated the difference between doses calculated and measured by TPS in a human cadaver with a hip prosthesis. As a result, their study found a significant difference between 17-33% between the measured and calculated doses for 140 points, depending on the thickness of the prosthesis[13]. Our current research found that Eclipse TPS significantly underestimated the dose at the hip prosthesis surface. Accordingly, this difference in the thick portion of the Co-Cr-Mo implant was 12.77% and 7.12% for the AAA and PBC algorithms, respectively. For Ti-6AI-4V alloy, this difference was 2.42%

and 6.09% for AAA and PBC algorithms, respectively. As can be seen from the measurement results, the differences between the values depend on the components of the implant, its internal structure, the material's electron density, and the implant's dimensions.

Rojas et al. compared dose distributions calculated by TPS and measured by TLDs for the adult pelvic phantom with a femoral prosthesis. Accordingly, a significant difference was found between the calculated and measured doses at the bone-metal interface. They found differences in the bone surface of the femur region of up to 12% and 150% for the left femur and right femur, respectively[14]. In our dosimetric study, a significant difference was found between the doses calculated by TPS at a 1.5 cm distance from the prosthesis and measured by TLD. Accordingly, the AAA and PBC algorithms underestimated 7.65% and 3.02% for Co-Cr-Mo. Also, for Ti-6AI-4V alloy, this difference was 6.79% and 9.47% for AAA and PBC algorithms, respectively.

Mohammadi et al. evaluated the accuracy of three different ISOgray treatment planning system algorithms in the presence of titanium and steel hip prostheses using Monte Carlo dose calculation. They found a difference of 24.78%, 27.68%, and 27.72% for the fast Fourier transform (FFT) convolution, collapsed cone (CC), and superposition in the 6 MV photon beam in the titanium implant, respectively. However, this difference was 32.84%, 35.89%, and 35.57% in the 6 MV photon beam in the steel implant, respectively[15]. Our current research is in line with the results of Mohammadi et al. The dose estimation performance of TPS decreased as the density of the implant increased. Accordingly, the difference between TPS and TLD doses is more in the presence of a Co-Cr-Mo prosthesis with a 6.89 g/cm^3 density.

Gul OV. et al. investigated the Eclipse AAA algorithm's surface dose calculation performance for intensity-modulated radiotherapy (IMRT) of head and neck cancer using TLDs. As a result of measurements taken at five different points, the AAA algorithm underestimated the surface dose by approximately 13.61%[16]. In our current study, a significant difference was found between the Eclipse TPS and TLD doses on the surface of the phantom. This difference was 12.44% and 24.91% for the AAA and PBC algorithms, respectively, in the presence of Co-Cr-Mo hip replacement. In addition, in the presence of Ti-6AI-4V alloy, it was 7.01% and 16.42% for AAA and PBC algorithms, respectively.

Studies comparing dose measurements in real hip prostheses in a tissue-equivalent phantom mimicking the leg are limited in the literature. In this dosimetric study, it was observed that Eclipse TPS could not accurately calculate backscatter in the presence of hip prostheses, and this would lead to uncertainties in the doses received by the patients. In addition, it is beneficial for TPS algorithms to evolve to remove these uncertainties constantly.

Conclusions

The accuracy of dose estimation of the Eclipse treatment planning system's AAA and PBC algorithms in the presence of hip prosthesis was investigated in a tissue-equivalent cylinder phantom in the X and Y axes using TLD dosimetry. It was observed that the uncertainty of the TPS algorithms increased as the density and diameter of the hip replacement increased. Therefore, in treating patients with hip replacement with radiation, it should be considered that the prosthesis may affect the treatment. Before the radiotherapy planning of patients with hip prostheses, the medical physicist should be informed about the electron density of the prosthesis. We recommend measuring entry and exit doses with TLDs in the first fraction to minimize the effect of the prosthesis on radiotherapy.

Ethical approval: Not required.

Acknowledgements: This study was supported by the Scientific Research Projects (BAP) Grants Unit, Selcuk University, Konya, TURKEY [Grant Number: 21401102].

REFERENCES

1. Antapur P, Mahomed N, Gandhi R. Fractures in the elderly: When is hip replacement a necessity? *Clin Interv Aging*. 2011;6:1-7. doi: 10.2147/CIA.S10204.

2. Wang Y. Current concepts in developmental dysplasia of the hip and total hip arthroplasty. *Arthroplasty*. 2019;1(1). doi: 10.1186/s42836-019-0004-6.

3. Rahmouni K, Besnard A, Oulmi K, Nouveau C, Hidoussi A, et al. In vitro corrosion response of CoCrMo and Ti-6Al-4V orthopedic implants with Zr columnar thin films. *Surface and Coatings Technology. 2022;436-444*. doi: 10.1016/j.surfcoat.2022.128310.

4. Abdul Aziz MZ, Mohd Kamarulzaman FN, Mohd Termizi NAS, Abdul Raof N, Tajuddin AA. Effects of density from various hip prosthesis materials on 6 MV photon beam: A Monte Carlo study. *Journal of Radiotherapy in Practice*. 2017;16(2):155-160. doi: 10.1017/s1460396917000012.

5. Palleri F, Baruffaldi F, Angelini AL, Ferri A, Spezi E. Monte Carlo characterization of materials for prosthetic implants and dosimetric validation of Pinnacle3 TPS. *Nuclear Instruments and Methods in Physics Research Section B: Beam Interactions with Materials and Atoms*. 2008;266(23):5001-5006. doi: 10.1016/j.nimb.2008.08.013.

6. Wellenberg RHH, Boomsma MF, Van Osch JAC, et al. Quantifying metal artefact reduction using virtual monochromatic dual-layer detector spectral CT imaging in unilateral and bilateral total hip prostheses. *European Journal of Radiology*. 2017;88:61-70. doi: 10.1016/j.ejrad.2017.01.002.

7. Çatlı S, Tanır G. Experimental and Monte Carlo evaluation of eclipse treatment planning system for effects on dose distribution of the hip prostheses. *Medical Dosimetry*. 2013;38(3):332-336. doi: 10.1016/j.meddos.2013.03.005.

8. De Martino F, Clemente S, Graeff C, Palma G, Cella L. Dose calculation algorithms for external radiation therapy: An overview for practitioners. *Applied Sciences*. 2021;11(15). doi: 10.3390/app11156806.

9. Flejmer AM, Dohlmar F, Nilsson M, Stenmarker M, Dasu A. Analytical anisotropic algorithm versus pencil beam convolution for treatment planning of breast cancer: Implications for target coverage and radiation burden of normal tissue. *Anticancer Res*. 2015;35(5):2841-2848.

10. Keehan S, Smith RL, Millar J, et al. Activation of hip prostheses in high energy radiotherapy and resultant dose to nearby tissue. *Journal of Applied Clinical Medical Physics*. 2017;18(2):100-105. doi: 10.1002/acm2.12058.

11. Paulu D, Alaei P. Evaluation of dose calculation accuracy of treatment planning systems at hip prosthesis interfaces. *Journal of Applied Clinical Medical Physics*. 2017;18(3):9-15. doi: 10.1002/acm2.12060.

12. Ojala J, Kapanen M, Sipilä P, Hyödynmaa S, Pitkänen M. The accuracy of Acuros XB algorithm for radiation beams traversing a metallic hip implant — comparison

with measurements and Monte Carlo calculations. *Journal of Applied Clinical Medical Physics*. 2014;15(5):162-176. doi: 10.1120/jacmp.v15i5.4912.

13. Le Fèvre C, Brinkert D, Menoux I, et al. Effects of a metallic implant on radiotherapy planning treatment—experience on a human cadaver. *Chinese Clinical Oncology*. 2020;9(2):14-14. doi: 10.21037/cco.2020.01.09.

14. Rojas DMC, Pavoni JF, Arruda GV, Baffa O. Gel and thermoluminescence dosimetry for dose verifications of a real anatomy simulated prostate conformal radiation treatment in the presence of metallic femoral prosthesis. *Journal of Applied Clinical Medical Physics*. 2021;22(10):278-287. doi: 10.1002/acm2.13403.

15. Mohammadi K, Hassani M, Ghorbani M, Farhood B, Knaup C. Evaluation of the accuracy of various dose calculation algorithms of a commercial treatment planning system in the presence of hip prosthesis and comparison with Monte Carlo. *Journal of Cancer Research and Therapeutics*. 2017;0(0). doi: 10.4103/0973-1482.204903.

16. Gul OV, Buyukcizmeci N, Basaran H. Evaluation of surface dose for intensity modulated radiotherapy of head and neck cancer using thermoluminescent dosimeters. *Gazi University Journal of Science Part A: Engineering and Innovation*. 2022;9(2):156-163. doi: 10.54287/gujsa.1109112.